Steven Franke and Niklas Neckel contributed equally to this work.

Key Points:

- Sentinel-1 DInSAR estimates reveal a ~175 km flow path of a cascade-like chain of subglacial water propagation over a 1-year period
- High-resolution ultra-wideband radar data show no characteristic lake bed reflections and suggests water transport via a local trough system
- We find evidence of highly dynamic water transport in a static glacial stetting providing a benchmark dataset to improve modeling results

Supporting Information:

Supporting Information may be found in the online version of this article.

Correspondence to:

N. Neckel,
niklas.neckel@awi.de

Evidence of Cascading Subglacial Water Flow at Jutulstraumen Glacier (Antarctica) Derived From Sentinel-1 and ICESat-2 Measurements

Niklas Neckel[1] ⓘ, Steven Franke[1] ⓘ, Veit Helm[1] ⓘ, Reinhard Drews[2] ⓘ, and Daniela Jansen[1] ⓘ

[1]Alfred Wegener Institute, Helmholtz Centre for Polar and Marine Research, Bremerhaven, Germany, [2]Department of Geosciences, Eberhard Karls University Tübingen, Tübingen, Germany

Abstract Migration of subglacial water underneath thick Antarctic ice is difficult to observe directly but is known to influence ice flow dynamics. Here, we analyze a 6-year time series of displacement maps from differential Sentinel-1 SAR interferometry (DInSAR) in the upstream region of Jutulstraumen Glacier. Our results reveal short-term (between 12 days and 1 year) interconnected subsidence- and uplift events of the ice surface, which we interpret as a pressure response to the drainage and filling of subglacial lakes. This indicates an episodic cascade-like water transport with longer quiescent phases in a dynamically stable glacial setting. Abrupt events appear in the DInSAR time series and are confirmed by ICESat-2 altimetry. The events can be traced for a 1-year period along a ~175 km flow path. We are able to observe the migration of subglacial water with unprecedented spatial and temporal resolution, providing a new observational baseline to further develop subglacial hydrological models.

Plain Language Summary Subglacial lakes and the movement of subglacial water play an important role in the way how ice flows in the Antarctic Ice Sheet. The drainage and filling of subglacial lakes is reflected in subsidence and uplift at the ice surface, which can be monitored by satellite based elevation measurements. In this study, we detect these elevation changes of the ice surface at the onset of Dronning Maud Land's largest glacier (Jutulstraumen Glacier, Antarctica). We register a number of connected events which show us where and when subglacial water moves downstream. We find that the water flows similarly to a self-tipping swimming pool bucket: water beneath the ice is localized and abruptly moves from one place to another after some time has passed. Using airborne radar-sounding techniques, we find that the water flows along preferential flowpaths in the subglacial system. These are the first confirmed subglacial water movements in central Dronning Maud Land, an area where no subglacial water flow has been observed previously. The episodic nature of water flow is a new observation that will help us to understand how the subglacial water forms its own pluming system beneath these large glaciers.

1. Introduction

Large quantities of basal meltwater are transported from the interior of the Antarctic Ice Sheet to downstream areas of faster ice flow, reducing the frictional resistance at the glacier bed (Joughin et al., 2004; Siegfried & Fricker, 2018). Subglacial water is known to pool in subglacial lakes and can be routed hundreds of kilometers along well-defined pathways (Fricker et al., 2014; Wingham et al., 2006). Indirect evidence of subglacial water movement was first detected by analyzing localized surface elevation changes of mountain glaciers (Capps et al., 2010; Fatland & Lingle, 2002; Iken et al., 1983). More recently, similar processes were also reported for the Greenland (Bowling et al., 2019; Howat et al., 2015; Willis et al., 2015) and Antarctic Ice Sheets (Fricker et al., 2007; Gray et al., 2005; Joughin et al., 2016; Spikes et al., 2003). Furthermore, it has been postulated that such events can not be treated as isolated phenomena but are interconnected through subglacial drainage networks (e.g., Ashmore & Bingham, 2014; Fricker et al., 2007).

Most observations of ice-surface uplift and subsidence are derived from satellite altimetry (e.g., Fricker et al., 2007; Siegfried & Fricker, 2018, 2021; Wingham et al., 2006), while a few studies also use Synthetic Aperture Radar (SAR) interferometry (e.g., Gray et al., 2005; Milillo et al., 2017) and SAR speckle tracking (e.g., Hoffman et al., 2020; Joughin et al., 2016). Subglacial lakes detected with these methods are often referred to as active lakes, in contrast to lakes solely detected using radio-echo sounding (RES), which may or

may not show temporal variations at the ice surface (Ashmore & Bingham, 2014). However, the detection of active lakes requires observation periods of months to years to coherently map ice surface elevation changes (Siegfried & Fricker, 2018). First studies indicate that the majority of active lakes are located beneath fast flowing ice streams in Antarctica (Fricker et al., 2014; Gray et al., 2005; Malczyk et al., 2020; Siegfried & Fricker, 2018; Smith et al., 2017). Goeller et al. (2016) found evidence for possible subglacial lake locations in Dronning Maud Land (DML) in RES data. However, no active lakes have been reported for central DML so far. Consequently, little is known about the subglacial hydrology, water transport and the impact on local ice dynamics (Thoma et al., 2012). In this study, we derive short-term changes in ice surface displacement lasting between 12 days and 1 year by means of differential SAR interferometry (DInSAR) on Sentinel-1 data. These displacement anomalies reveal a cascade-like pattern starting in the onset region of Jutulstraumen Glacier (JG, Figure 1). Additional ICESat-2 repeat-track measurements capture more gradual elevation changes at the same locations lasting for up to 1 year. However, when integrating the DInSAR displacements over the repeat period of ICESat-2, we find similar results for both datasets. This indicates vertical movement of the ice surface, which we interpret as filling and drainage of subglacial lakes. We further use a dense grid of ultra-wideband (UWB) RES data to obtain detailed information about the bed topography. The combination of these datasets indicates that the subglacial water transport generally follows the hydraulic gradient and migrates downstream in a localized trough system.

2. Study Site

Jutulstraumen Glacier is the largest ice draining glacier in DML. Ice flows from the polar plateau to the lower coastal section of the East Antarctic Ice Sheet (EAIS) and follows the bearing of the Jutulstraumen Graben through the DML escarpment (Andersen et al., 2020). The JG trough is 40–50 km wide, 1.6 km below present sea level (Fretwell et al., 2013) at its deepest location, and ice flow velocity accelerates to 760 m a^{-1} at the grounding line (Mouginot et al., 2019). Our survey area is located at the onset of JG where ice flow is convergent and accelerating from 5 to 100 m a^{-1} (Figure 1c). Possible locations for subglacial lakes have been reported in central DML by Goeller et al. (2016). However, their analysis is solely based on radio-echo sounding (RES) surveys and the potential lake locations are restricted to the margins of the JG drainage basin. Ice thickness and bed topography have been extensively mapped in this region (Ferraccioli et al., 2005; Riedel et al., 2012; Steinhage et al., 1999, 2001) and indicate a spatially variable and preserved alpine landscape, which has been most likely generated by relief-controlled glacial erosion, sub-aerial weathering and fluvial erosion from mountain glaciers (Franke et al., 2021; Näslund, 2001).

3. Data and Methods

In order to detect localized vertical ice-surface displacements we employed satellite borne estimates from Sentinel-1 InSAR and ICESat-2 laser altimetry. To complement our findings, we used airborne radar data and the REMA DEM for high-resolution mapping of the hydropotential. The applied datasets and methods are described in the following.
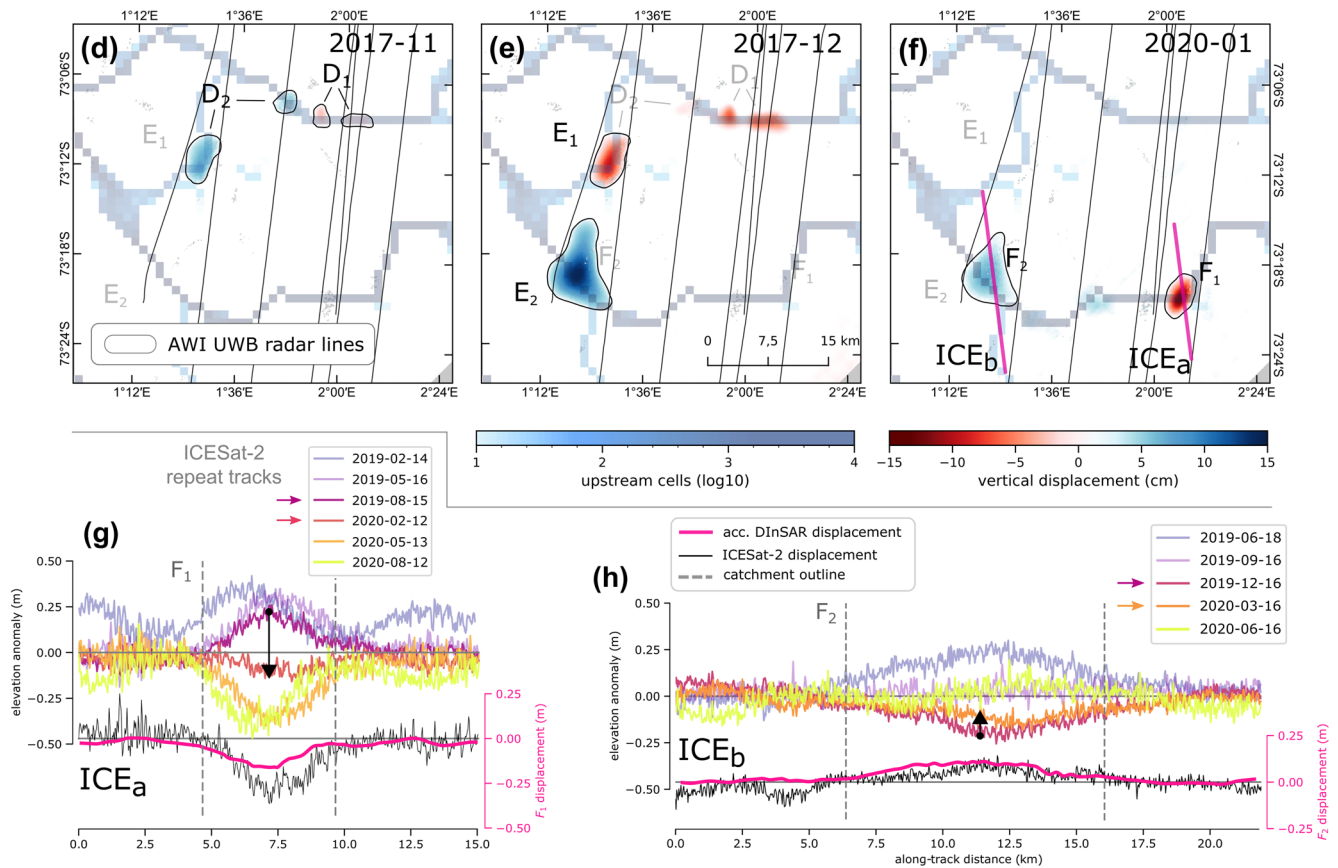
3.1. Ice-Surface Displacements

We applied InSAR processing to Sentinel-1 Interferometric Wide (IW) swath mode data to detect anomalous surface displacements in the satellite's Line Of Sight (LOS). We highlight local anomalies over short time scales by canceling the background ice flow using double-differences as commonly done for grounding line estimates (e.g., Friedl et al., 2020; Joughin et al., 2016; Rignot et al., 2011; Figures 1d –1f). We computed 247 double-differential interferograms between 2015-05 and 2020-09, covering large parts of our study region (Figure 1b). Steady horizontal displacements were removed from the time series by (a) subtracting two interferograms from a 12-day baseline and (b) calculating the anomaly with respect to an average multi-year interferogram (Text S1 and Figure S1). As the majority of the interferograms showed no bull's-eye fringe patterns, method (b) was more suitable for isolating the vertical displacement and better constrains the timing of the events. Hence, all vertical DInSAR displacement values throughout this manuscript are based on the long-term displacement anomaly with unwrapped results projected from LOS to vertical (e.g., Figures 2d–2f). The fact that most double-differential interferograms showed no anomalous fringe patterns
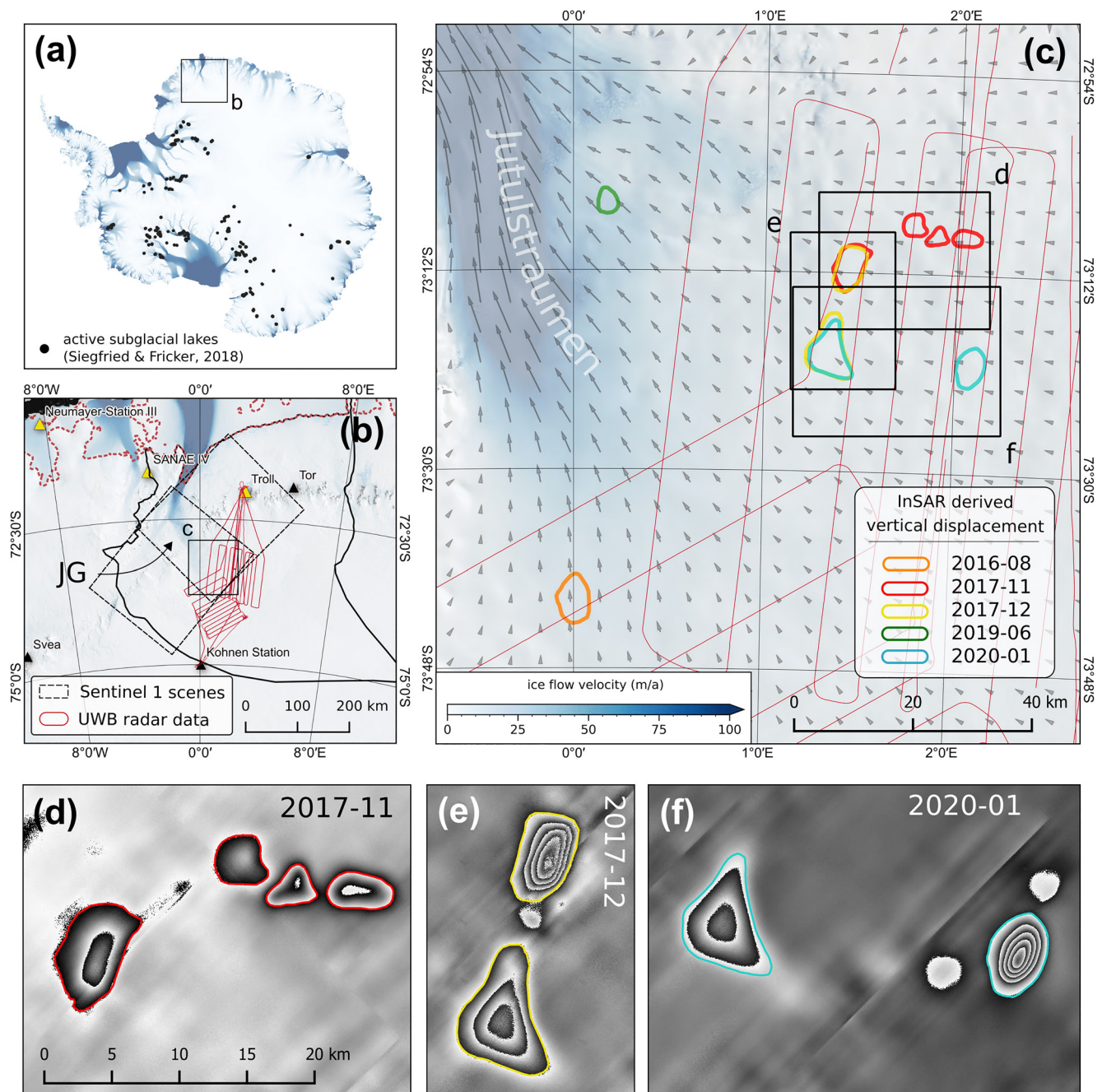
Figure 1. Overview of: (a) the locations of active subglacial lakes in Antarctica (Siegfried & Fricker, 2018), (b) central/western DML with the drainage basin of Jutulstraumen Glacier (JG), (c) locations of DInSAR detected displacement anomalies of the ice surface at the onset of JG and (d)–(f) differential interferograms of three events indicating coupled displacement of the ice surface. Ice surface velocities in (a)–(c) are obtained from Mouginot et al. (2019) and the boundaries of the drainage system in (b) are from Mouginot & Rignot (2017) and Rignot et al. (2013).

either in the form of distinct bull's-eyes nor in the downstream direction of the drainage events is picked up later to discriminate potential large-scale changes in horizontal ice flow velocities. In addition, we used data from the Advanced Topographic Laser Altimeter System carried on board the Ice, Cloud and land Elevation Satellite-2 (ICESat-2) to find elevation anomalies over the DInSAR-detected events. We employed level 3A Land Ice Height (ATL06) Version 3 data (Smith et al., 2019), which are available for the time period starting on October 14, 2018 (Smith et al., 2020). We modified the repeat-track analysis approach introduced by Fricker et al. (2014) to address the data acquisition characteristics specific to ICESat-2 (six beams instead of

Figure 2. Vertical displacement of the ice surface derived from DInSAR and ICESat-2 repeat track elevation changes. Panels (d)–(f) show the events D, E, and F, which are computed from the anomaly to a long-term average interferogram. The transparent blue gridcells represent the subglacial water routing pathways based on the number of upstream cells. The gray lines show the locations of the AWI UWB (ultra-wideband) radar lines. Panel (f) shows the locations of the ICESat-2 tracks shown in (g) and (h). Track ICE_a corresponds to RGT 0732 GT3l and ICE_b to RGT 1235 GT1r. Elevation anomalies (difference to the mean) for multiple ICESat-2 repeat passes are shown in (g) and (h). The cumulated DInSAR anomalies between the time periods indicated by the arrows are shown in the lower part of (g) and (h) together with the difference of the time-consistent ICESat-2 anomalies (black curve).

one nadir beam; Text S2). Based on this analysis, we were able to detect elevation changes over the locations of the DInSAR-detected bull's-eye fringe patterns (Figures 2g and 2h). In this study, we used ICESat-2 data with the Reference Ground Track (RGT) 0732 and Ground Track (GT) GT3l as well as RGT 1235 and GT1r (see Text S2 for details).

3.2. Hydropotential Mapping

The DInSAR-detected bull's-eye fringe patterns in Figures 1d–1f are also covered by multiple airborne radar data profiles. The data were acquired at the onset region of JG during the austral summer of 2018/19, using a multichannel ultra-wide band (UWB) radar system operated by the Alfred Wegener Institute, Helmholtz Center for Polar and Marine Research (AWI; Figures 1b and 1c; Franke et al., 2021). The radar system comprises an array of eight antenna elements installed underneath the fuselage a BT-67 aircraft. All radar profiles were recorded at a center frequency of 195 MHz and a bandwidth of 30 MHz (180–210 MHz). We provide a description of the specific acquisition geometry and corresponding radar processing steps (Text S3) and refer to Hale et al. (2016) and Rodriguez-Morales et al. (2014) for further system specifics. The radar data cover areas that are not covered in Antarctic-wide ice thickness and bed topography maps (Fretwell et al., 2013; Morlighem et al., 2020), and we include this additional information to resolve the bed in our area of interest in finer detail (see also Franke et al., 2021, for further details on the data and methods used for the refined bed topography). The grid size of our refined bed topography is 1 km.

For mapping preferential water flow paths, we used the locally improved bed topography and the Reference Elevation Model of Antarctica (REMA, Howat et al., 2019) to estimate the glaciological hydraulic potential in our study area (e.g., Shreve, 1972; Smith et al., 2017). A flow accumulation grid was generated on the basis of the depression filled refined bed topography using the algorithm proposed by Tarboton (1997) (Text S4). In this approach, flow direction is defined from the steepest downward slope in the hydraulic potential of each pixel's eight triangular facets. The output is displayed as the number of up-slope grid cells (Figures 2d–2f).

4. Results

From our time series of 247 DInSAR estimates, we find at least three time periods of significant LOS surface displacement within spatially limited regions (Figures 1d–1f). These events are labeled as event D in November 2017 (Figure 1d), event E in December 2017 (Figure 1e), and event F in January 2020 (Figure 1f). Maximum vertical surface displacements range between 4.1 and 14.4 cm within the 12 days repeat pass of Sentinel-1 (Table S1). All events are clustered in an area of approx. 1,000 km^2 and are located 225 km upstream the grounding line of JG. The individual areas of these bull's-eye-shaped events range from 17 to 93 km^2 (Table S1). We find a spatial overlap of event D and E, as well as E and F. The duration of subsidence and uplift ranges between 12 days for event D_2/E_1 and up to 1 year for event F_1 (Figure 2).

In addition to the three main events described above, we detected several smaller displacement events with maximum surface displacement magnitudes between ~2 and 6 cm (Figures S2 and S3). These smaller events occur close to the region of the main events D, E and F and can be observed during two time periods: 2017-09 to 2018-08 (Figure S2) and 2019-09 to 2020-03 (Figure S3). Unwrapping clearly distinguishes subsidence from uplift allowing the spatial and temporal links between individual events to become apparent (Figure 2, Movie S1). Also the time period of <1 month for filling and draining is significantly shorter as for the larger events. The first additional event appeared in 2017-09 and is located ~50 km northeast of event E_1. Subsequent events (including D and E) occur increasingly downstream [as time progresses] (Figure 3). A synthesis of all events results in a ~175 km-long chain along which successive subsidence and uplift occurs throughout the time series. The second period between 2019-11 and 2020-02 is characterized by a similar pattern but is more restricted to the upstream area (Figure S3). In order to detect changes in ice flow velocities, we carefully checked the single InSAR displacement estimates downstream the potential active lake locations. An example is shown in Figure S4b where InSAR LOS displacements are shown along a flowline originating from event location E_2/F_2 (Figure S4a). While both events are clearly visible in the time series (marked by black arrows in Figure S4b) no anomalous surface displacements are detected further downstream.

The temporal sampling of ICESat-2 data restricts our investigation to elevation anomalies along repeated ground tracks intersecting the outlines of event F_1 and F_2 (Figure 2f). Here, we find spatial overlaps for the time period between 2019-02 and 2020-06. We observe ice surface elevation changes for two ICESat-2 tracks (see Figures 2g and 2h). Track ICE_a (Figure 2g) shows constant subsidence adding up to more than 0.7 m between 2019-02–14 and 2020-08-12 in the region F_1. The elevation changes from track ICE_b (Figure 2h) also indicate gradual ice surface subsidence between 2019-06-18 and 2019-12-16 in the region F_2. Thereafter, we observe an uplift until 2020-06-15, when the mean elevation level is reached again. The maximum elevation anomaly is found in the center of the target regions F_1 and F_2. This applies for both positive and negative values. The elevation anomalies approach zero toward the area margins.

To integrate our DInSAR results with the ICESat-2 analysis we show the cumulative sum of the DInSAR time series within the respective repeat pass periods along the ICESat-2 tracks ICE_a and ICE_b (Figures 2g and 2h). We selected two time periods from our DInSAR time series which closely match the ICESat-2 repeat passes (indicated by the arrows in Figures 2g and 2h) and find a good agreement between ICESat-2 and the cumulative DInSAR displacement. Figure 2 shows the subglacial water routing pathways together with the individual events of the DInSAR-derived vertical elevation changes. All identified areas of subsidence or uplift spatially coincide with [interconnected] subglacial water routing pathways. The improved bed topography reveals that the areas of ice uplift and subsidence are mostly related to topographic depressions (Figure 3). The bed topography depressions associated with events D_2/E_1 and E_2/F_1 also coincide with sinks
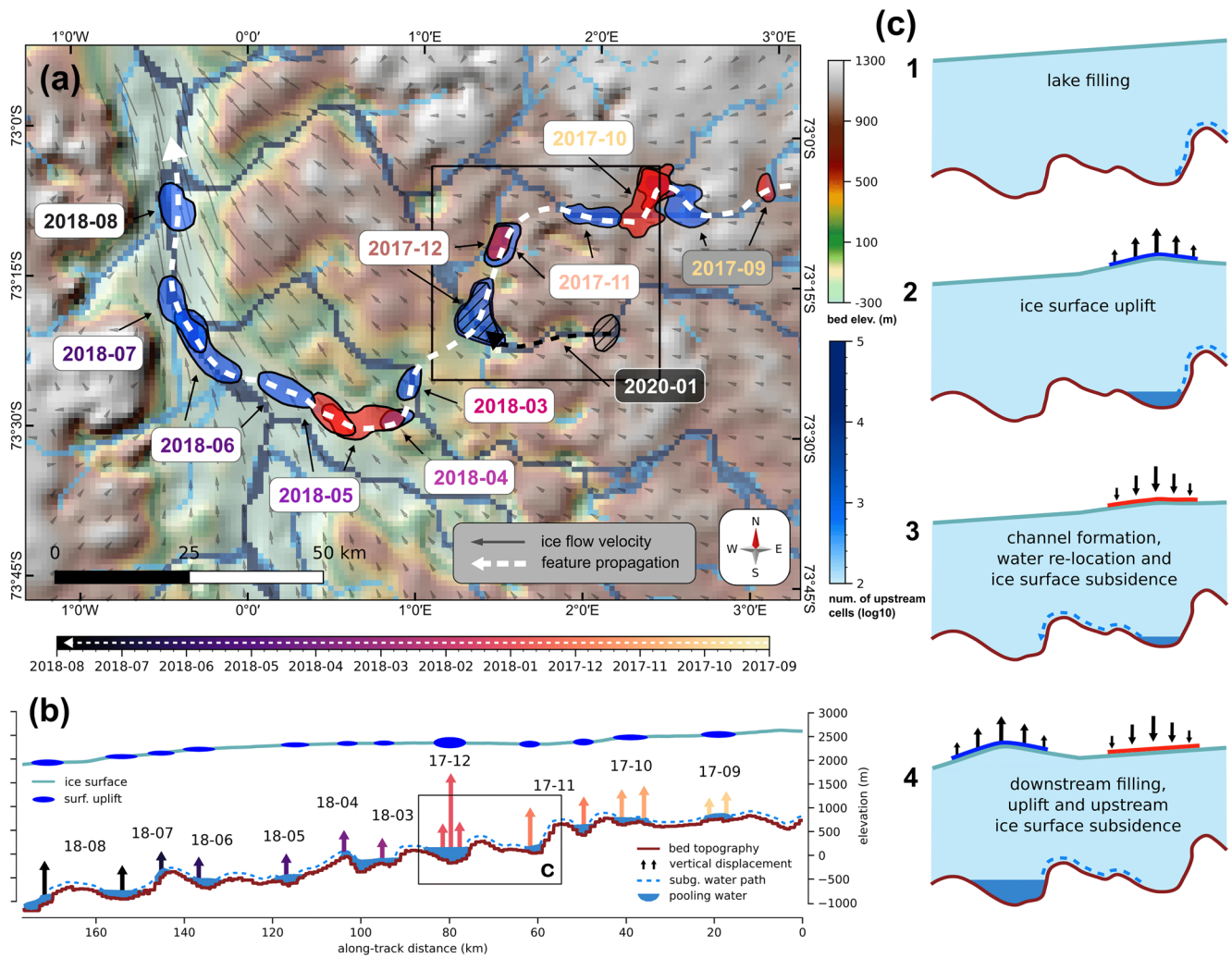
Figure 3. Spatio-temporal propagation of ice surface uplift and subsidence events. Panel (a) shows selected areas of uplift (blue) and subsidence (red) for each month between 2017-09 and 2018-08. Ice surface flow velocity is shown with gray arrows and ranges from $2 - 175 \, \mathrm{m \, a^{-1}}$. The complete time series is available in Figure S2 and Movie S1. Panel (b) shows the initial uplift events for each location. The propagation of subglacial water along the bed is indicated with a blue dashed line as well as the filling of local sinks. The pressure-related uplift is indicated with upright arrows with the respective color for the timing. The length of the arrow is proportional to the maximum uplift. The DInSAR-detected uplift at the ice surface is indicated with a blue outline. Panel (c) indicates the temporal sequence of filling and drainage of two adjacent sinks and the respective response at the ice surface.

in the hydraulic potential (Figure S8a). Most events are located over V-shaped valleys (see Figures S5, S6, and S8), the depth of which constantly increases from (hydrologically) upstream to downstream.

5. Discussion

Building on previous large-scale studies based on satellite altimetry (e.g., Fricker et al., 2007; Siegfried & Fricker, 2018, 2021), the combination of Sentinel-1 and ICESat-2 measurements offers new insights into the inter-connectivity of subglacial lake drainage events. Here we present a highly resolved chain-like pattern stretching from the onset of JG toward the grounding line (Figures 3a and 3b, Movie S1). The setting of JG is such that the subglacial water generated in the large upstream catchment must be funneled through a comparatively narrow constriction starting at the ice-stream onset. This favors the development of efficient channelized drainage systems similar to what has been observed at other ice streams (e.g., at Recovery Ice Stream, Dow et al., 2018). Our observations indicate that this drainage is not steady but contains episodic events of locally increased water storage resulting in negative effective pressure manifested in localized surface uplift. After sufficient build-up, the pressure then abruptly changes in a way that facilitates more

downstream transport of water to a different low in the hydraulic potential where this process is then re-iterated (Figures 3b and 3c). These observations are in line with previous modeling based assertions (Dow et al., 2018) and observational studies at Recovery (Fricker et al., 2014) and Thwaites Glacier (Hoffman et al., 2020; Smith et al., 2017).

The proposed mechanism indicates that water is efficiently transported via transient channels. Whether these channels are Röthlisberger channels that melt into the ice (Dow et al., 2018) or subglacial canals incised into the sediments (Carter et al., 2017) remains open to discussion. The idea of a channelized drainage system with efficient water transport is further supported by the observed lack of large-scale changes in ice flow dynamics after the drainage events (Figure S4). However, here we have to admit that the geometry of the available SAR acquisitions is rather unfavorable for mapping ice velocities as the main ice flow direction is close to the azimuth direction of the satellite. Therefore, these estimates are restricted to the sensitivity of the SAR sensor.

Instead of following the prevailing ice flow direction, the chain of interconnected DInSAR anomalies largely follows the hydraulic gradient (Figure 3a). Small deviations from the hydraulic gradient can be attributed to several reasons: (1) uncertainties in ice surface elevation or bed topography (Figure S7b), (2) the assumption that basal water pressure equals the ice overburden pressure might not hold true in all places, (3) interpolation artifacts in the input datasets influence the accuracy of the derived hydraulic potential (e.g., data gaps in the ice thickness data, Figures S7a and S8b), (4) algorithm artifacts caused by the choice of the flow routing algorithm (Desmet & Govers, 1996), and (5) the sink filling algorithm might flatten some regions and hence can also impact the subglacial routing pathways.

In comparison to the lakes found in this study, most active lakes so far detected in Antarctica are clustered in regions of elevated ice flow velocity and are subject to larger lake volume changes (Smith et al., 2009; Siegfried & Fricker, 2018, 2021). The latter is also reflected in the timing and duration of the drainage events. During the 2017/2018 chain of events the duration of the drainages varied between 12 days (Sentinel-1 repeat pass time, event E_1) and ~5 months (events E_2 and D_1) along its 175 km flowpath. The cascading chain of events is therefore not linear but dependent on basin size with the largest basin taking up to 2 months (event E_2) of filling before draining. The 2019/2020 drainage events can not be followed as far downstream as during the 2017/2018 chain of events. In 2019/2020, the longest period of lake drainage was found for lake F_1, which showed a drainage duration of ~1 year, which is in accordance with both DInSAR and ICESat-2 estimates (Figure 2g). The duration of the drainage events is significantly shorter than reported from ICESat measurements elsewhere in Antarctica (Fricker & Scambos, 2009; Fricker et al., 2007). However, also lake size and drainage magnitudes are smaller than in the above studies.

To our knowledge, this is the first study, which finds active lakes in central DML. However, this might be attributed to the fact that compared to the altimetry measurements of previous studies, InSAR is not restricted to sparse repeat tracks and is capable of detecting surface elevation changes at the wavelength scale of the sensor. This makes DInSAR sensitive to small drainage events, which are possibly not resolved in altimetry based estimates. Such highly resolved DInSAR time series both in space and time will also be of great value for other regions in Antarctica where indirect measurements of small scale elevation changes are missing so far, but will improve our knowledge of local drainage systems and are of great value to inform modeling studies (e.g., Napoleoni et al., 2020).

Many locations where active subglacial lakes have been identified using satellite altimetry have also been surveyed by airborne RES campaigns (e.g., Christianson et al., 2012; Humbert et al., 2018; Siegert et al., 2014; Wright et al., 2012), which did not identify any characteristic [strong, flat and specular] bed reflection at the lake sites (Carter et al., 2007). Such reflections are also absent in our study region and sometimes the bed reflection is absent completely, which may be due to several factors such as high englacial attenuation rates, which reduce the receiving signal power. Since englacial attenuation is a function of temperature, it is possible that warm ice in the troughs underneath our active lake catchments or a temperate layer of basal ice might be the cause for the reduction in, and in some cases total absence of, basal reflectivity (Humbert et al., 2018; Siegert et al., 2014). Christianson et al. (2012) and Siegert et al. (2014) argue that, in order to create a dielectric contrast of 10–20 dB higher than the surrounding material, a minimum water table of several meters' thickness is required. However, our centimeter-scale elevation changes combined with the

odds of a radar survey coinciding with a filled lake (Siegert et al., 2014), strongly indicate that RES-based detection of subglacial water is very unlikely in our survey area (see Figures S5 and S6). This agrees with the lack of evidence for a deep water lake at JG. Nonetheless, it may still be possible that larger-than-anticipated amounts of subglacial water are being transported. Carter et al. (2017) showed that subglacial lakes in Antarctica could drain through sediment-floored canals, which might serve as a further explanation for the missing evidence in the RES data.

6. Summary and Outlook

We identified a subglacial hydrologic network at Jutulstraumen Glacier in which subglacial water is periodically trapped and released. We are able to trace the propagation of subglacial water over a distance of ~175 km within 1 year using a combination of different remote sensing methods. DInSAR estimates from Sentinel-1 data reveal abrupt but localized events occurring between 12 days and 1 year. Individual events are interconnected in a cascade-like pattern of short-term surface uplift and subsidence following lows in the hydraulic potential indicating an episodic transport of excess water across subglacial lakes. ICESat-2 repeat-tracks capture the long-term lake drainage patterns and match with the cumulated DInSAR displacements, but undersample the short term dynamics. Additional airborne radar data constrains the hydraulic potential and show that the inter-connected chain of subsidence and uplift events occurs along projected pathways of subglacial water flux. The subglacial water is not apparent in the bed reflection amplitudes either due to its transient nature or because of a lack in system sensitivity. Despite the widely discussed influence of subglacial water on local ice flow variability, we find no evidence of associated changes in downstream ice velocities from the DInSAR dataset. The lake areas and surface displacement magnitudes found in this study are relatively small and could only be detected due to the high spatial and temporal resolution of the Sentinel-1 DInSAR estimates. This enabled us to find evidence of highly dynamic water transport in a rather static glacial setting. Such findings might now also be possible for other slow moving areas in Antarctica where no water movement was detected before. Our results contribute to the understanding of the subglacial hydrology of Antarctica in regions with small scale water movements, where observations were not possible so far. This knowledge gain will be valuable for improving hydrological models and is needed to capture the entire spectrum of hydrological processes.

Data Availability Statement

Sentinel-1 SAR data are freely available from https://scihub.copernicus.eu. ICESat-2 level 3A land ice height data are freely available from https://nsidc.org/data/atl06/versions/3. The center coordinates of active lake locations derived in this study are available in the Supplementary Material. Outlines and locations of the lakes and processed ICESat-2 tracks are available at the PANGAEA repository (Neckel et al. (2021); https://doi.pangaea.de/10.1594/PANGAEA.927120). Ice thickness from the AWI UWB radar survey (Franke et al., 2020) is available at https://doi.pangaea.de/10.1594/PANGAEA.911475. Ice surface velocities from Mouginot et al. (2019) are available at the National Snow and Ice Data Center (NSIDC), https://doi.org/10.7280/D10D4Z. The REMA ice surface DEM (Howat et al., 2019) is available from the U.S. Polar Geospatial Center at https://www.pgc.umn.edu/data/rema/. The drainage system boundaries (Rignot et al., 2013) can be obtained here: https://doi.org/10.5067/AXE4121732AD. The inventory of subglacial lakes was provided by M. Siegfried.

References

Andersen, J., Newall, J., Blomdin, R., Sams, S., Fabel, D., Koester, A., et al. (2020). Ice surface changes during recent glacial cycles along the Jutulstraumen and Penck trough ice streams in western Dronning Maud Land, East Antarctica. *Quaternary Science Reviews*, *249*, 106636. https://doi.org/10.1016/j.quascirev.2020.106636

Ashmore, D., & Bingham, R. G. (2014). Antarctic subglacial hydrology: Current knowledge and future challenges. *Antarctic Science*, *26*, 758–773. https://doi.org/10.1017/S0954102014000546

Bowling, J. S., Livingstone, S. J., Sole, A. J., & Chu, W. (2019). Distribution and dynamics of Greenland subglacial lakes. *Nature Communications*, *10*(1), 2810. https://doi.org/10.1038/s41467-019-10821-w

Capps, D. M., Rabus, B., Clague, J. J., & Shugar, D. H. (2010). Identification and characterization of alpine subglacial lakes using interferometric synthetic aperture radar (InSAR): Brady Glacier, Alaska, USA. *Journal of Glaciology*, *56*(199), 861–870. https://doi.org/10.3189/002214310794457254

Carter, S. P., Blankenship, D. D., Peters, M. E., Young, D. A., Holt, J. W., & Morse, D. L. (2007). Radar-based subglacial lake classification in Antarctica. *Geochemistry, Geophysics, Geosystems*, *8*(3), 1–20. https://doi.org/10.1029/2006gc001408

Carter, S. P., Fricker, H. A., & Siegfried, M. R. (2017). Antarctic subglacial lakes drain through sediment-floored canals: Theory and model testing on real and idealized domains. *The Cryosphere*, *11*(1), 381–405. https://doi.org/10.5194/tc-11-381-2017

Christianson, K., Jacobel, R. W., Horgan, H. J., Anandakrishnan, S., & Alley, R. B. (2012). Subglacial Lake Whillans — ice-penetrating radar and GPS observations of a shallow active reservoir beneath a West Antarctic Ice Stream. *Earth and Planetary Science Letters*, *331–332*, 237–245. https://doi.org/10.1016/j.epsl.2012.03.013

Desmet, P. J. J., & Govers, G. (1996). Comparison of routing algorithms for digital elevation models and their implications for predicting ephemeral gullies. *Geographical Information Systems*, *10*(3), 311–331. https://doi.org/10.1080/026937996138061

Dow, C. F., Werder, M. A., Babonis, G., Nowicki, S., Walker, R. T., Csatho, B., & Morlighem, M. (2018). Dynamics of active subglacial lakes in recovery ice stream. *Journal of Geophysical Research: Earth Surface*, *123*(4), 837–850. https://doi.org/10.1002/2017jf004409

Fatland, D. R., & Lingle, C. S. (2002). InSAR observations of the 1993–95 bering glacier (Alaska, U.S.A.) surge and a surge hypothesis. *Journal of Glaciology*, *48*(162), 439–451. https://doi.org/10.3189/172756502781831296

Ferraccioli, F., Jones, P. C., Curtis, M. L., & Leat, P. T. (2005). Subglacial imprints of early Gondwana break-up as identified from high resolution aerogeophysical data over western Dronning Maud Land, East Antarctica. *Terra Nova*, *17*(6), 573–579. https://doi.org/10.1111/j.1365-3121.2005.00651.x

Franke, S., Eisermann, H., Jokat, W., Eagles, G., Asseng, J., Miller, H., & Jansen, D. (2021). Preserved landscapes underneath the Antarctic Ice Sheet reveal the geomorphological history of Jutulstraumen Basin. Earth Surface Processes and Landforms, 46(13), 2728–2745. https://doi.org/10.1002/esp.5203

Franke, S., Jansen, D., & Helm, V. (2020). *Ice thickness from Jutulstraumen Glacier recorded with the airborne AWI UWB radar system, Antarctica*. PANGAEA. https://doi.org/10.1594/PANGAEA.911475

Fretwell, P., Pritchard, H. D., Vaughan, D. G., Bamber, J. L., Barrand, N. E., Bell, R., et al. (2013). Bedmap2: Improved ice bed, surface and thickness datasets for Antarctica. *The Cryosphere*, *7*(1), 375–393. https://doi.org/10.5194/tc-7-375-2013

Fricker, H. A., Carter, S. P., Bell, R. E., & Scambos, T. (2014). Active lakes of recovery ice stream, east antarctica: A bedrock-controlled subglacial hydrological system. *Journal of Glaciology*, *60*(223), 1015–1030. https://doi.org/10.3189/2014JoG14J063

Fricker, H. A., & Scambos, T. (2009). Connected subglacial lake activity on lower Mercer and Whillans Ice Streams, West Antarctica, 2003–2008. *Journal of Glaciology*, *55*(190), 303–315. https://doi.org/10.3189/002214309788608813

Fricker, H. A., Scambos, T., Bindschadler, R., & Padman, L. (2007). An active subglacial water system in West Antarctica mapped from space. *Science*, *315*(5818), 1544–1548. https://doi.org/10.1126/science.1136897

Friedl, P., Weiser, F., Fluhrer, A., & Braun, M. H. (2020). Remote sensing of glacier and ice sheet grounding lines: A review. *Earth-Science Reviews*, *201*, 102948.

Goeller, S., Steinhage, D., Thoma, M., & Grosfeld, K. (2016). Assessing the subglacial lake coverage of Antarctica. *Annals of Glaciology*, *57*(72), 109–117. https://doi.org/10.1017/aog.2016.23

Gray, L., Joughin, I., Tulaczyk, S., Spikes, V. B., Bindschadler, R., & Jezek, K. (2005). Evidence for subglacial water transport in the West Antarctic Ice Sheet through three-dimensional satellite radar interferometry. *Geophysical Research Letters*, *32*(3), 1–4. https://doi.org/10.1029/2004GL021387

Hale, R., Miller, H., Gogineni, S., Yan, J. B., Leuschen, C., Paden, J., & Li, J. (2016). *MULTI-channel ultra-wideband radar sounder and imager center for remote sensing of ice Sheets*. Germany: University of Kansas Alfred Wegener InstituteIEEE International Geoscience and Remote Sensing Symposium (IGARSS).

Hoffman, A. O., Christianson, K., Shapero, D., Smith, B. E., & Joughin, I. (2020). Brief communication: Heterogenous thinning and subglacial lake activity on Thwaites Glacier, West Antarctica. *The Cryosphere*, *14*(12), 4603–4609.

Howat, I. M., Porter, C., Noh, M. J., Smith, B. E., & Jeong, S. (2015). Brief Communication: Sudden drainage of a subglacial lake beneath the Greenland Ice Sheet. *The Cryosphere*, *9*(1), 103–108. https://doi.org/10.5194/tc-9-103-2015

Howat, I. M., Porter, C., Smith, B. E., Noh, M.-J., & Morin, P. (2019). The reference elevation model of Antarctica. *The Cryosphere*, *13*(2), 665–674. https://doi.org/10.5194/tc-13-665-2019

Humbert, A., Steinhage, D., Helm, V., Beyer, S., & Kleiner, T. (2018). Missing evidence of widespread subglacial lakes at recovery glacier, Antarctica. *Journal of Geophysical Research: Earth Surface*, *123*(11), 2802–2826. https://doi.org/10.1029/2017jf004591

Iken, A., Röthlisberger, H., Flotron, A., & Haeberli, W. (1983). The uplift of unteraargletscher at the beginning of the melt season—A consequence of water storage at the bed? *Journal of Glaciology*, *29*(101), 28–47. https://doi.org/10.3189/s0022143000005128

Joughin, I., Shean, D. E., Smith, B. E., & Dutrieux, P. (2016). Grounding line variability and subglacial lake drainage on Pine Island Glacier, Antarctica. *Geophysical Research Letters*, *43*(17), 9093–9102. https://doi.org/10.1002/2016gl070259

Joughin, I., Tulaczyk, S., MacAyeal, D. R., & Engelhardt, H. (2004). Melting and freezing beneath the Ross ice streams, Antarctica. *Journal of Glaciology*, *50*(168), 96–108. https://doi.org/10.3189/172756504781830295

Malczyk, G., Gourmelen, N., Goldberg, D., Wuite, J., & Nagler, T. (2020). Repeat subglacial lake drainage and filling beneath Thwaites Glacier. *Geophysical Research Letters*, *47*(23), e2020GL089658. https://doi.org/10.1029/2020gl089658

Milillo, P., Rignot, E., Mouginot, J., Scheuchl, B., Morlighem, M., Li, X., & Salzer, J. T. (2017). On the short-term grounding zone dynamics of Pine Island Glacier, West Antarctica, observed with COSMO-SkyMed interferometric data. *Geophysical Research Letters*, *44*(20), 436–510. https://doi.org/10.1002/2017gl074320.10444

Morlighem, M., Rignot, E., Binder, T., Blankenship, D., Drews, R., Eagles, G., & Young, D. A. (2020). Deep glacial troughs and stabilizing ridges unveiled beneath the margins of the Antarctic ice sheet. *Nature Geoscience*, *13*(2), 132–137. https://doi.org/10.1038/s41561-019-0510-8

Mouginot, J., Scheuchl, B., Rignot, E. (2017). *MEaSUREs Antarctic boundaries for IPY 2007-2009 from satellite radar, Version 2*. https://doi.org/10.5067/AXE4121732AD10.5067/AXE4121732AD

Mouginot, J., Rignot, E., & Scheuchl, B. (2019). Continent-wide, interferometric SAR phase, mapping of Antarctic ice velocity. *Geophysical Research Letters*, *46*(16), 9710–9718. https://doi.org/10.1029/2019GL083826

Napoleoni, F., Jamieson, S. S. R., Ross, N., Bentley, M. J., Rivera, A., Smith, A. M., & Vaughan, D. G. (2020). Subglacial lakes and hydrology across the Ellsworth Subglacial Highlands, West Antarctica. *The Cryosphere*, *14*(12), 4507–4524. https://doi.org/10.5194/tc-14-4507-2020

Näslund, J. O. (2001). Landscape development in western and central Dronning Maud Land, East Antarctica. *Antarctic Science*, *13*(3), 302–311. https://doi.org/10.1017/S0954102001000438

Neckel, N., Franke, S., & Helm, V. (2021). *Locations, outlines and ICESat-2 tracks of active lakes at the onset of the Jutulstraumen Glacier (Antarctica)*. PANGAEA. https://doi.org/10.1594/PANGAEA.927120

Riedel, S., Jokat, W., & Steinhage, D. (2012). Mapping tectonic provinces with airborne gravity and radar data in Dronning Maud Land, East Antarctica. *Geophysical Journal International*, *189*(1), 414. https://doi.org/10.1111/j.1365-246X.2012.05363.x

Rignot, E., Jacobs, S., Mouginot, J., & Scheuchl, B. (2013). Ice-shelf melting around Antarctica. *Science*, *341*(6143), 266–270. https://doi.org/10.1126/science.1235798

Rignot, E., Mouginot, J., & Scheuchl, B. (2011). Antarctic grounding line mapping from differential satellite radar interferometry. *Geophysical Research Letters*, *38*(10), 6. https://doi.org/10.1029/2011gl047109

Rodriguez-Morales, F., Gogineni, S., Leuschen, C. J., Paden, J. D., Li, J., Lewis, C. C., et al. (2014). Advanced multifrequency radar instrumentation for polar research. *IEEE Transactions on Geoscience and Remote Sensing*, *52*(5), 2824–2842. https://doi.org/10.1109/TGRS.2013.2266415

Shreve, R. L. (1972). Movement of water in Glaciers. *Journal of Glaciology*, *11*(62), 205–214. https://doi.org/10.3189/S002214300002219X

Siegert, M. J., Ross, N., Corr, H., Smith, B., Jordan, T., Bingham, R. G., & Le Brocq, A. (2014). Boundary conditions of an active West Antarctic subglacial lake: Implications for storage of water beneath the ice sheet. *The Cryosphere*, *8*(1), 15–24. https://doi.org/10.5194/tc-8-15-2014

Siegfried, M. R., & Fricker, H. A. (2018). Thirteen years of subglacial lake activity in Antarctica from multi-mission satellite altimetry. *Annals of Glaciology*, *59*(76pt1), 42–55. https://doi.org/10.1017/aog.2017.36

Siegfried, M. R., & Fricker, H. A. (2021). Illuminating active subglacial lake processes with ICESat-2 laser altimetry. *Geophysical Research Letters*, *48*(14), e2020GL091089. https://doi.org/10.1029/2020GL091089

Smith, B., Fricker, H., Gardner, A., Siegfried, M. S. A., & Csathó, B. (2020). ATLAS/ICESat-2 L3A Land Ice Height, Version 3. Boulder, Colorado USA. The ICESat-2 science Team. NASA National Snow and Ice Data Center Distributed Active Archive Center. https://doi.org/10.5067/ATLAS/ATL06.003

Smith, B., Fricker, H. A., Holschuh, N., Gardner, A. S., Adusumilli, S., Brunt, K. M., & Siegfried, M. R. (2019). Land ice height-retrieval algorithm for NASA's ICESat-2 photon-counting laser altimeter. *Remote Sensing of Environment*, *233*, 111352. https://doi.org/10.1016/j.rse.2019.111352

Smith, B. E., Fricker, H. A., Joughin, I. R., & Tulaczyk, S. (2009). An inventory of active subglacial lakes in Antarctica detected by ICESAT (2003–2008). *Journal of Glaciology*, *55*(192), 573–595. https://doi.org/10.3189/002214309789470879

Smith, B. E., Gourmelen, N., Huth, A., & Joughin, I. (2017). Connected subglacial lake drainage beneath Thwaites Glacier, West Antarctica. *The Cryosphere*, *11*(1), 451–467. https://doi.org/10.5194/tc-11-451-2017

Spikes, V. B., Csatho, B. M., Hamilton, G. S., & Whillans, I. M. (2003). Thickness changes on Whillans Ice Stream and Ice Stream c, West Antarctica, derived from laser altimeter measurements. *Journal of Glaciology*, *49*(165), 223–230. https://doi.org/10.3189/172756503781830683

Steinhage, D., Nixdorf, U., Meyer, U., & Miller, H. (1999). New maps of the ice thickness and subglacial topography in Dronning Maud Land, Antarctica, determined by means of airborne radio-echo sounding. *Annals of Glaciology*, *29*, 267–272. https://doi.org/10.3189/172756499781821409

Steinhage, D., Nixdorf, U., Meyer, U., & Miller, H. (2001). Subglacial topography and internal structure of central and western Dronning Maud Land, Antarctica, determined from airborne radio echo sounding. *Journal of Applied Geophysics*, *47*(3–4), 183–189. https://doi.org/10.1016/S0926-9851(01)00063-5

Tarboton, D. G. (1997). A new method for the determination of flow directions and upslope areas in grid digital elevation models. *Water Resources Research*, *33*(2), 309–319. https://doi.org/10.1029/96wr03137

Thoma, M., Grosfeld, K., Mayer, C., & Pattyn, F. (2012). Ice-flow sensitivity to boundary processes: A coupled model study in the Vostok Subglacial Lake area, Antarctica. *Annals of Glaciology*, *53*(60), 173–180. https://doi.org/10.3189/2012AoG60A009

Willis, M. J., Herried, B. G., Bevis, M. G., & Bell, R. E. (2015). Recharge of a subglacial lake by surface meltwater in northeast Greenland. *Nature*, *518*(7538), 223–227. https://doi.org/10.1038/nature14116

Wingham, D. J., Siegert, M. J., Shepherd, A., & Muir, A. S. (2006). Rapid discharge connects Antarctic subglacial lakes. *Nature*, *440*(7087), 1033–1036. https://doi.org/10.1038/nature04660

Wright, A. P., Young, D. A., Roberts, J. L., Schroeder, D. M., Bamber, J. L., Dowdeswell, J. A., & Siegert, M. J. (2012). Evidence of a hydrological connection between the ice divide and ice sheet margin in the Aurora Subglacial Basin, East Antarctica. *Journal of Geophysical Research*, *117*(F1), F01033. https://doi.org/10.1029/2011JF002066